The H 2 O 2 -Resistant Fe–S Redox Switch MitoNEET Acts as a pH Sensor To Repair Stress-Damaged Fe–S Protein

Cécile Mons, Thomas Botzanowski, Anton Nikolaev, Petra Hellwig, Sarah Cianférani, Ewen Lescop, Cécile Bouton, Marie-Pierre Golinelli

Biochemistry
Article
Cite This: Biochemistry XXXX, XXX, XXX−XXX
pubs.acs.org/biochemistry

The H_2O_2-Resistant Fe−S Redox Switch MitoNEET Acts as a pH Sensor To Repair Stress-Damaged Fe−S Protein

Cécile Mons,[†] Thomas Botzanowski,[‡] Anton Nikolaev,[§] Petra Hellwig,[§] Sarah Cianférani,[‡] Ewen Lescop,[†] Cécile Bouton,[†] and Marie-Pierre Golinelli-Cohen*[,†]

[†]Institut de Chimie des Substances Naturelles, CNRS UPR 2301, Univ Paris-Sud, Université Paris-Saclay, 91198 Gif-sur-Yvette cedex, France

[‡]Laboratoire de Spectrométrie de Masse BioOrganique, Université de Strasbourg, CNRS, IPHC UMR 7178, 67000 Strasbourg, France

[§]Laboratoire de Bioélectrochimie et Spectroscopie, UMR 7140, Chimie de la Matière Complexe, Université de Strasbourg-CNRS, 1 rue Blaise Pascal, 67000 Strasbourg, France

Supporting Information

ABSTRACT: Human mitoNEET (mNT) is the first identified Fe−S protein of the mammalian outer mitochondrial membrane. Recently, we demonstrated the involvement of mNT in a specific cytosolic pathway dedicated to the reactivation of oxidatively damaged cytosolic aconitase by cluster transfer. *In vitro* studies using apo-ferredoxin (FDX) reveal that mNT uses an Fe-based redox switch mechanism to regulate the transfer of its cluster. Using the "gold standard" cluster recipient protein, FDX, we show that this transfer is direct and that only one of the two mNT clusters is transferred when the second one is decomposed. Combining complementary biophysical and biochemical approaches, we show that pH affects both the sensitivity of the cluster to O_2 and dimer stability. Around physiological cytosolic pH, the ability of mNT to transfer its cluster is tightly regulated by the pH. Finally, mNT is extremely resistant to H_2O_2 compared to ISCU and SufB, two other Fe−S cluster transfer proteins, which is consistent with its involvement in a repair pathway of stress-damaged Fe−S proteins. Taken together, our results suggest that the ability of mNT to transfer its cluster to recipient proteins is not only controlled by the redox state of its cluster but also tightly modulated by the pH of the cytosol. We propose that when pathophysiological conditions such as cancer and neurodegenerative diseases dysregulate cellular pH homeostasis, this pH-dependent regulation of mNT is lost, as is the regulation of cellular pathways under the control of mNT.

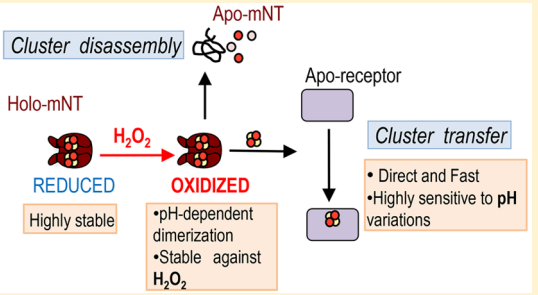

Iron−sulfur (Fe−S) clusters are evolutionarily ancient and highly conserved prosthetic cofactors. Composed of only iron and sulfur, they are involved in many essential biological processes.[1,2] MitoNEET (mNT), also known as CISD1, is the first identified Fe−S protein of the mammalian outer mitochondrial membrane (OMM).[3,4] This is a small homodimeric protein (13 kDa for each monomer) anchored to the OMM by its 32-amino acid N-terminus with the major part of the protein, including the C-terminal Fe−S binding domain, located in the cytosol.[4] Each monomer accommodates one [2Fe-2S] cluster coordinated by three cysteines (C72, C74, and C83) and one histidine (H87) in a CDGSH domain[5−8] as other members of the NEET protein family,[9] which also includes Miner1 (or CISD2) and Miner2 (or CISD3) in mammals.[10] Although the biological activity of mNT is still debated,[11] studies have shown that it is involved in the regulation of iron/reactive oxygen species homeostasis,[12−14] in the regulation of lipid and glucose metabolism,[13,15] and in cell proliferation in breast cancer.[16]

In vitro studies revealed that holo-mNT (the form of the protein with the cluster) is able to transfer its Fe−S cluster to very diverse apoprotein (an Fe−S protein, which has lost its cluster) recipients assembling either a [2Fe-2S] cluster as ferredoxin from various organisms,[17,18] human anamorsin[19] and CISD2,[20] or a [4Fe-4S] cluster as mammalian iron regulatory protein-1 (IRP-1)/cytosolic aconitase (c-aconitase).[14] On the basis of *in cellulo* experiments, we showed that mNT is able to repair the oxidatively damaged Fe−S cluster of human IRP-1/c-aconitase by transferring its cluster to the damaged protein.[14]

Recently, we started to investigate in depth the *in vitro* cluster transfer reaction, focusing on the transfer from holo-mNT to [2Fe-2S] recipient protein. We unambiguously demonstrated that oxidized mNT ($[2Fe\text{-}2S]^{2+}$) triggers cluster transfer, whereas reduction of its cluster abrogates this transfer. Moreover, while O_2 significantly affects the lability of the oxidized mNT cluster, it does not interfere with the cluster

Received: July 20, 2018
Revised: August 22, 2018

DOI: 10.1021/acs.biochem.8b00777
Biochemistry XXXX, XXX, XXX−XXX

transfer reaction. Thus, in contrast to the strict anoxia required for other Fe−S cluster transfer proteins such as ISCU, mNT is able to transfer its cluster even under aerobic conditions. The reduced form of mNT is extremely stable compared to the oxidized form, even though no major change in overall protein folding was found by NMR studies between these two redox states of the protein.[17] Thus, when reduced, mNT is in a dormant physiological state, while oxidative insults oxidize its cluster and switch it to an active state ready to initiate Fe−S transfer. Then, we proposed that mNT belongs to the new family of Fe−S proteins acting as a redox switch to control the adaptive cellular response after oxidative stress insult.[21] Recently, it was proposed that anamorsin might act as a regulator of mNT by transferring an electron to oxidized mNT and switching it to the reduced dormant state when oxidant stress is no longer present.[22]

In the study presented here, we pursue the *in vitro* characterization of the mNT cluster transfer reaction to a [2Fe-2S] recipient protein, apo-FDX, which is the "gold standard" used in various laboratories to study [2Fe-2S] cluster transfer processes.[17,18,23−30] We show that this transfer is a direct process and mNT transfers only one of its clusters to apo-FDX when the second one is decomposed. Combining different complementary biophysical and biochemical approaches, we show that pH affects both cluster coordination and vicinity and dimer stability, and maybe more importantly, it induces a tight regulation of the cluster transfer reaction around physiological values. Finally, we show that mNT is extremely resistant to H_2O_2 compared to other Fe−S cluster transfer proteins such as IscU and SufB, in agreement with our proposed involvement of mNT in cluster repair after stress.

MATERIALS AND METHODS

Purifications of Holo-mNT$_{44–108}$ and Apo-FDX. As described previously,[14] a construct missing the 43 N-terminal amino acids (mNT$_{44–108}$) was expressed in fusion with a His tag at the C-terminal end of pET22b. Consequently, the purified mNT$_{44–108}$ form contains eight additional C-terminal residues derived from the His tag (LEHHHHHH) and will be named mNT herein. Holo-FDX was expressed from the pET21b plasmid (gift from S. Ollagnier de Choudens, Grenoble, France). Holo-mNT$_{44–108}$ and holo-FDX were expressed and purified as described previously.[23] The protein purity was assessed to be >99% using sodium dodecyl sulfate−polyacrylamide gel electrophoresis (SDS−PAGE). For the WT form of holo-mNT, the optical A_{280}/A_{458} ratio was near 2.3. Apo-FDX was prepared by heat cluster disassembly of purified holo-FDX in the presence of 10 mM dithiothreitol (DTT) and 10 mM ethylenediaminetetraacetic acid (EDTA) followed by purification on a NAP-5 column (GE Healthcare) equilibrated with 50 mM Tris-HCl (pH 7.0) and 100 mM NaCl.[23]

For NMR analyses, expression of ^{15}N- and ^{13}C-labeled mNT$_{44–108}$ was performed on a 1 L scale in M9 minimal medium (containing 0.001% thiamine-HCl and 10 μM $FeCl_3$), supplemented with 1.0 g of $^{15}NH_4Cl$ and 4.0 g of [^{13}C]-D-glucose as the sole nitrogen and carbon sources, respectively.

Protein concentrations were measured using Bradford's assay with bovine serum albumin (BSA) as the standard[31] or the absorbance at 280 nm of guanidine-denatured protein using values of 7115 and 7365 M^{-1} cm^{-1} (ProtParam) as extinction coefficients for mNT$_{44–108}$ and FDX, respectively. All protein concentrations were calculated on the basis of monomer equivalents.

***In Vitro* mNT Cluster Loss and Transfer Reactions.** Except for native mass spectrometry, reaction buffers were all composed of 100 mM NaCl and 50 mM MES (pH 4.6 and 5.4), Bis-Tris (pH 5.8, 6.2, and 6.7), or Tris-HCl (pH >7.0). Native mass spectrometry studies were performed in 50 mM $AcONH_4$ (pH 5.8 or 6.7).

For cluster transfer reactions, apo-FDX was preincubated with 5 mM DTT for 30 min at room temperature under anaerobic conditions to ensure cysteine reduction. When specified, DTT was removed and buffer was exchanged to cluster transfer reaction buffer using a Micro Bio-Spin Size Exclusion column (Bio-Rad). Disassembled mNT (apo-mNT) was prepared by incubation of the protein in pH 6.2 reaction buffer at 65 °C for 10 min. Chemical Fe−S cluster reconstitution in FDX was performed in 50 mM Bis-Tris (pH 6.2), 100 mM NaCl, with 100 μM Na_2S and ammonium iron(II) sulfate (Mohr's salt) or iron chloride ($FeCl_3$) for 2 h at 25 °C under aerobic conditions. Reactions were followed by native mass spectrometry, ultraviolet−visible (UV−vis) absorption and NMR spectroscopies, or migration of aliquots taken at specific times (1 mM DTT was added to the samples before migration) on a 16% native PAGE gel colored with colloidal Coomassie staining as described in ref 23. $T_{1/2}$ is defined as the time required for half of the reaction to proceed. When necessary, protein gels were quantified using an Odyssey Imaging System (LI-COR Biosciences) and the percentage of holo-FDX was calculated as the ratio of the intensity of the holo-FDX band to the sum of the intensities of apo- and holo-FDX bands.

UV−Vis Absorption and NMR Spectroscopy Studies. UV−vis absorption spectra were recorded between 240 and 900 nm with a Cary 100 (Agilent) or Safas mc^2 (Monaco) spectrophotometer equipped with a temperature control apparatus set to the desired temperature. For spectra taken under anaerobic conditions, the cuvette was prepared in a glovebox and closed with a septum.

NMR experiments were performed using a Bruker Avance III 800 MHz spectrometer equipped with a TCI cryoprobe. Two-dimensional (2D) ^{1}H−^{15}N band-selective optimized flip angle short transient heteronuclear multiple-quantum correlation (SOFAST-HMQC) spectra[32] were recorded using a 100 μM His-tagged ^{15}N- and ^{13}C-labeled holo-mNT$_{44–108}$ protein sample at 298 K in the specified buffers. UV−vis absorption and NMR spectroscopies were used as described in ref 23 to follow cluster loss and cluster transfer reactions.

Iron Quantification. Free and total irons were quantified using a bathophenanthroline colorimetric assay adapted from refs 33 and 34. For total iron quantification of a 100 μL protein sample, 10 μL of 54% perchloric acid was added. After 30 min at room temperature, 72 μL of 1.7 mg/mL bathophenanthroline sulfonate, 18 μL of 76 mg/mL sodium ascorbate, and 10 μL of a saturated ammonium acetate solution were added, and the reaction mixture was supplemented with water until the volume reached 350 μL. After 30 min at room temperature, the absorbance at 535 nm was measured. Free iron quantification was performed using the same protocol except that perchloric acid was not added and 250 μL of protein sample was used.

Raman Spectroscopy. Raman spectra were recorded on a Renishaw in Via Raman Microscope equipped with a charge-coupled device detector at 15 °C. Samples were excited with the 457 nm line of an argon laser where the output power was set to 16.5 mW. The output power was varied depending on the signal intensity. Small protein droplets of 1 μL were

DOI: 10.1021/acs.biochem.8b00777
Biochemistry XXXX, XXX, XXX−XXX

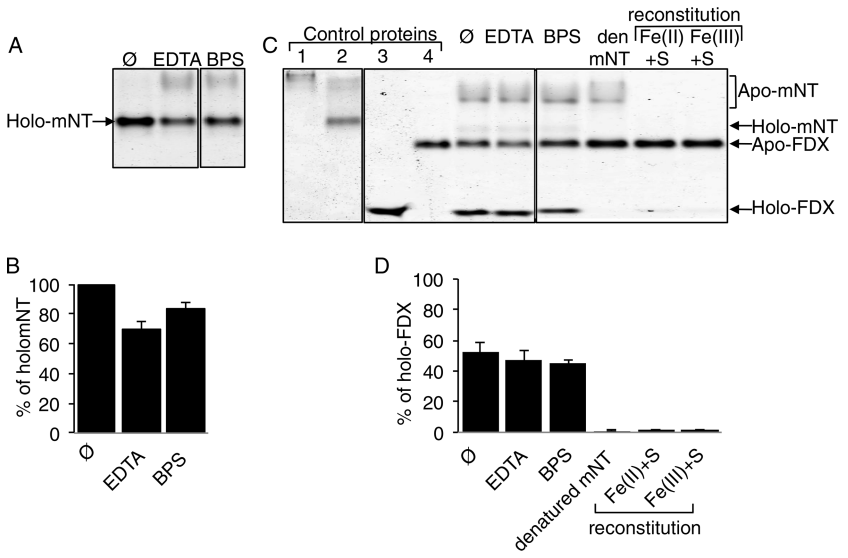

Figure 1. mNT cluster transfer is a direct process. Cluster transfer reactions were performed with 50 μM oxidized holo-mNT and apo-FDX in 50 mM Bis-Tris (pH 6.2) and 100 mM NaCl at 25 °C under aerobic conditions for 2 h. Reaction products were separated on a 16% reducing native gel (A and C). The histograms are the average of at least two independent experiments (B and D). (A and B) Holo-mNT was incubated at 25 °C for 2 h with 250 μM EDTA and 100 μM BPS or without an additive (Ø). Reaction products were analyzed on a 16% reducing native gel (A), and the percentage of holo-mNT was calculated from the intensities of bands corresponding to holo- and apo-mNT (B). (C and D) Cluster transfer reactions were performed with 250 μM EDTA and 100 μM BPS or without an additive (Ø). Lane den mNT represents a reaction mixture containing apo-FDX and disassembled mNT (den mNT) prepared as described in Materials and Methods. Chemical reconstitution of the FDX cluster in the presence of 100 μM Na_2S and either 100 μM Mohr's salt [lane Fe(II)+S] or 100 μM iron chloride [lane Fe(III)+S] was also tried under the same conditions (pH 6.2 under aerobic conditions). Apo-mNT (lane 1), holo-mNT (lane 2), holo-FDX (lane 3), and apo-FDX (lane 4) were loaded as migration controls. Reaction products were analyzed on a 16% reducing native gel (C), and the percentage of holo-FDX was calculated from the intensities of the bands corresponding to holo-FDX and apo-FDX (D).

deposited on a polyethylene window and dried with a stream of argon. Approximately 400 accumulations were averaged with an exposure time of 10 s, for each sample.

Electrochemically Induced FTIR Difference Spectroscopy. The ultra-thin layer spectroelectrochemical cell was used as described previously.[35] To avoid irreversible protein adhesion, the gold grid working electrode was modified overnight with hexanethiol and 6-mercapto-1-hexanol and rinsed with ethanol and then with water. To accelerate the redox reactions, a mixture of 19 mediators[36] was added in a substoichiometric concentration of 40 μM each to the protein solution; 7−8 μL of the protein solution was used to fill the electrochemical cell. The cell path length was <10 μm, as determined at the beginning of each experiment. All experiments were performed at 278 K.

FTIR spectra were recorded as a function of the applied potential using a setup combining an IR beam from the interferometer (Vertex 70, Bruker) for the 4000−1000 cm^{-1} range. First, the protein was equilibrated at an initial electrode potential, and a single-beam spectrum was recorded. Then, the final potential was applied, and a single-beam spectrum was again recorded after equilibration. Equilibration generally took <4 min for the full potential step from −0.6 to 0 V (Ag/AgCl). Difference spectra as presented here were calculated from two single-beam spectra, with the initial spectrum taken as a reference. Typically, 2 × 256 interferograms at 4 cm^{-1} resolution were co-added for each single-beam spectrum and Fourier transformed using triangular apodization and a zero filling factor of 2. At least 60 difference spectra were averaged.

Chemicals and Preparation of Protein Samples for Mass Spectrometry Analysis. Chemicals were from Sigma-Aldrich: ammonium acetate ($AcONH_4$, catalog no. A1542) and high-performance liquid chromatography-grade acetonitrile (catalog no. 34851). Aqueous solutions were prepared using an ultrapure water system (Sartorius, Göttingen, Germany). Before native mass spectrometry experiments, mNT_{44-108} storage buffer was exchanged with a 50 mM $AcONH_4$ solution at pH 5.8 or pH 6.7 using Zeba Spin Desalting Columns with a 7 kDa molecular weight cutoff (Thermo Fisher Scientific). The protein concentration was determined by the UV absorbance using a NanoDrop spectrophotometer (Thermo Fisher Scientific).

Denaturing and Native Mass Spectrometry Analysis. Native mass spectrometry measurements were performed in positive ion mode on an electrospray time-of-flight mass spectrometer (LCT, Waters, Manchester, U.K., upgraded by MS Vision) equipped with an automated chip-based nanoESI source (Triversa Nanomate, Advion). The instrument was calibrated using multiply charged ions of a 2 μM horse heart myoglobin solution. For analysis under denaturing conditions, samples were diluted to 20 μM for infusion in a 1/1 (v/v) water/acetonitrile mixture acidified with 0.5−1% formic acid and interface parameters were fixed to 45 V for accelerating voltage (Vc) and 2 mbar for backing pressure (bP) to obtain the best mass accuracy. Under these conditions, noncovalent interactions in WT mNT were typically disrupted allowing the measurement of the molecular weight of the apo-mNT_{44-108} monomer with good accuracy ($M_{W\ Exp}$ = 8577.8 ± 0.1 Da; $M_{W\ Theo}$ = 8577.8 Da for the WT form).

Analyses under native conditions were performed after careful optimization of instrumental settings to avoid dissociation of noncovalent bonds and to obtain sensitive detection of protein/iron−sulfur clusters. Vc and bP were fixed to 20 V and 6 mbar, respectively. Protein was diluted to 20 μM

DOI: 10.1021/acs.biochem.8b00777
Biochemistry XXXX, XXX, XXX−XXX

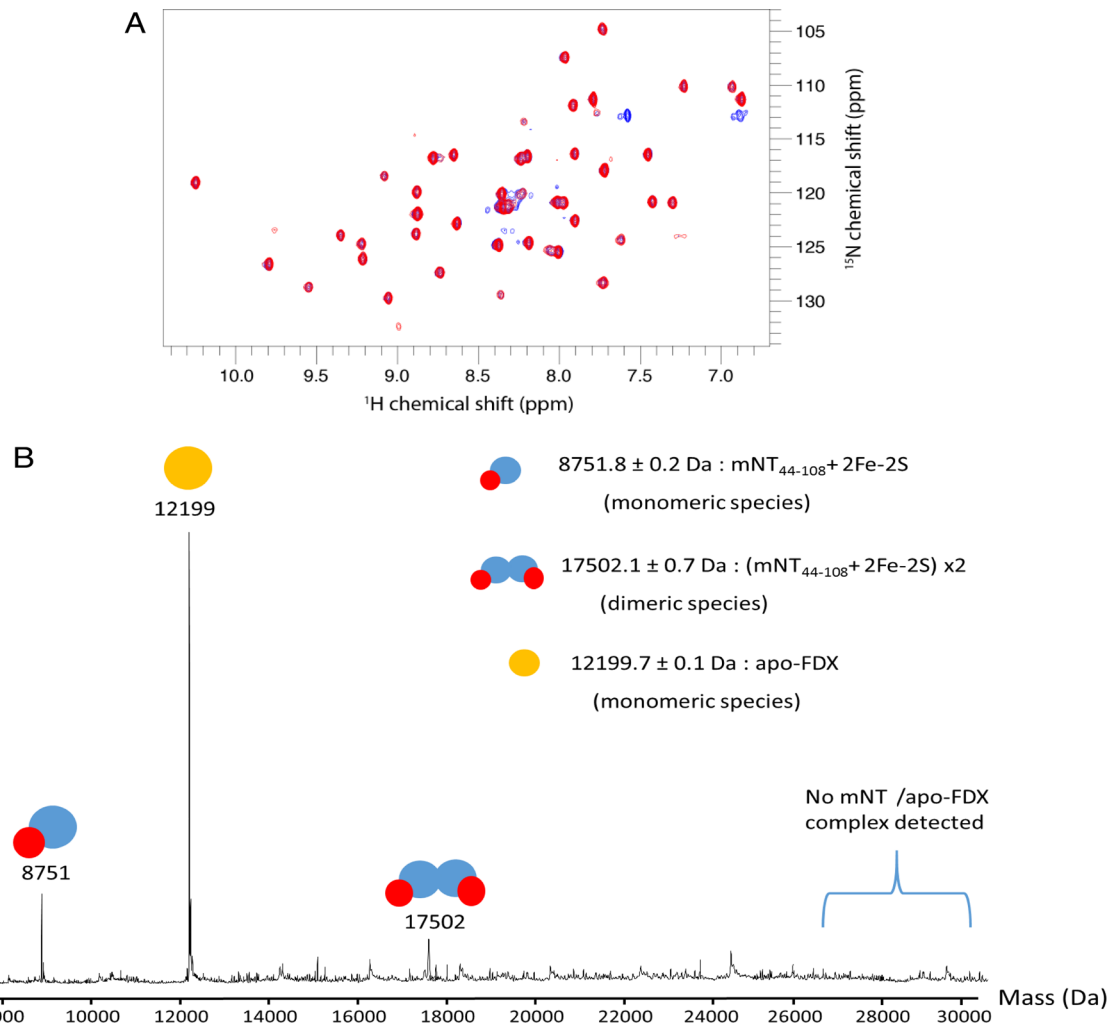

Figure 2. Oxidized holo-mNT and apo-FDX do not form a stable complex. (A) Overlay of ^{15}N SOFAST-HMQC spectra of 100 μM ^{15}N- and ^{13}C-labeled oxidized holo-mNT in the absence (red) or presence (blue) of 100 μM apo-FDX in 50 mM Tris-HCl (pH 6.7) and 100 mM NaCl at 298 K collected under aerobiosis. All holo-mNT crosspeaks can be superimposed under both conditions, suggesting very limited or no molecular interaction between holo-mNT and apo-FDX. The additional crosspeaks visible in the presence of FDX are due to the apo-mNT form, which accumulates after cluster transfer. (B) Deconvoluted electrospray mass spectra obtained under native conditions of 20 μM holo-mNT in the presence of 20 μM apo-FDX in 50 mM $AcONH_4$ (pH 6.7) at room temperature. No complex between apo-FDX and holo-mNT was detected under our experimental conditions.

in $AcONH_4$ (pH 5.8 or 6.7). Native MS experiments were performed in triplicate under identical conditions at 0, 0.5, 1, 2, 3, and 4 h at room temperature. Acquisitions were performed in the mass range of m/z 20−5000 with a 4 s scan time. Data analysis was performed with MassLynx version 4.0 (Waters, Manchester, U.K.).

RESULTS

mNT Cluster Transfer Is a Direct Process. First, we looked at the nature of the cluster transfer reaction between holo-mNT and the recipient protein. Does it occur directly or through a two-step mechanism with disassembly of the mNT cluster followed by reassembly of a cluster in FDX? Previously, we found that cluster transfer is much faster than cluster disassembly under exactly the same reaction conditions (protein concentrations, temperature, and buffer). Moreover, cluster transfer was not affected by oxygen, unlike cluster stability.[17] These previous results suggest that cluster transfer might be direct. To unambiguously demonstrate its nature, we looked at the effects of the addition of ferric [ethylenediaminetetraacetic acid (EDTA)] or ferrous [bathophenanthroline sulfonate (BPS)] ion chelators on the products of the transfer reaction under aerobic conditions. Products were analyzed after reaction for 2 h, a sufficient time for the reaction to reach completion under our conditions (Figure 1). If the mNT cluster has to be disassembled prior to reassembly in FDX, then addition of an iron chelator would inhibit the formation of a cluster in FDX. At concentrations of chelators (250 μM EDTA and 100 μM BPS) that do not lead to significant holo-mNT destabilization (Figure 1A,B), the amount of formed holo-FDX at the end of the reaction was not affected compared to those of reactions performed in the absence of an iron chelator (in panels C and D of Figure 1, compare lanes EDTA and BPS with lane Ø). Nevertheless, a pink coloration was readily observed (data not shown) when the cluster transfer reaction was performed in the presence of BPS, indicating iron release (the complex of BPS with iron is pink) during the reaction. In contrast, when the mNT cluster was disassembled prior to the addition of apo-FDX, no cluster insertion in FDX was observed (Figure 1C,D, lane den mNT).

DOI: 10.1021/acs.biochem.8b00777
Biochemistry XXXX, XXX, XXX−XXX

Finally, the Fe−S cluster could not be inserted in apo-FDX by simple addition of iron as ferric or ferrous ions and inorganic sulfur (chemical cluster reconstitution) under the same reaction conditions (pH, temperature, concentrations, and aerobic conditions) (Figure 1C,D, reconstitution lanes). Thus, the cluster transfer from holo-mNT to apo-FDX is unambiguously a direct process.

mNT and FDX Did Not Form a Stable Complex. Previous studies based on a protein−protein complex docking model and protein cross-linking had shown that CISD2 could form a complex with FDX.[11] First, we questioned if the formation of a stable complex between donor and acceptor proteins is required for the cluster to be transferred or if a transient complex is sufficient. Thus, we studied the potential molecular interaction by protein pull-down using purified mNT (in fusion with a His tag) and FDX in apo and holo forms. No direct interaction between these two proteins was observed using this technique (data not shown). NMR spectroscopy is another powerful technique for probing molecular interactions and was successfully used to highlight the interaction between mNT and anamorsin.[22] Indeed, NMR chemical shifts and peak line shapes are highly sensitive to changes in environment and mobility, and one would expect spectral perturbations of mNT NMR spectra upon addition of apo-FDX if the bimolecular complex is significantly populated in solution. Two different NMR tubes were prepared at pH 8.0 containing 100 μM ^{15}N- and ^{13}C-labeled oxidized mNT with or without 100 μM unlabeled apo-FDX, and the solutions were then solvent-exchanged to decrease the pH to 6.7 prior to NMR data collection under aerobic conditions. Under these conditions, cluster transfer occurs slowly with a $T_{1/2}$ of >10 h. The 2D ^{15}N SOFAST-HMQC spectra collected just after the pH jump are shown in Figure 2A. In the absence of apo-FDX (red spectrum), the ^{1}H-^{15}N 2D spectrum is typical of oxidized holo-mNT.[14] When apo-FDX was also present (blue spectrum), the oxidized holo-mNT state dominated the spectra and had chemical shifts and a peak line shape virtually identical to those of the spectrum collected in the absence of apo-FDX. This strongly suggests little interaction between the two proteins under these conditions. The additional peaks visible in the presence of apo-FDX correspond to the apo-mNT[14] that starts to accumulate because of cluster transfer before the recording of the first NMR spectra (*vide infra*). Finally, binding between holo-mNT (20 μM) and apo-FDX (20 μM) was studied at pH 6.7 by native mass spectrometry (MS), a method allowing preservation of protein−protein and protein−metal ion interactions.[37−39] Again, no heterocomplex involving both proteins was observed under these experimental conditions, and only signals of unbound apo-FDX and holo-mNT were detected (Figure 2B). Taken together, pull-down, NMR, and native MS studies demonstrate that apo-FDX and oxidized holo-mNT do not form a high-affinity complex prior to cluster transfer but only a transient complex as observed by chemical cross-linking in the case of CISD2 with FDX.[11] Thus, only the formation of a transient, but not stable, complex between donor and acceptor proteins is required for cluster transfer.

Only One Cluster of Dimeric mNT Is Transferred to Apo-FDX. In previously published transfer reaction experiments performed with equimolar donor and acceptor proteins,[17,18] it was observed that roughly 50% of apo-FDX was converted to holo-FDX when all holo-mNT had lost its cluster, suggesting that only half of available clusters from holo-mNT were transferred to the recipient protein assembling one [2Fe-2S]. Moreover, the pink coloration that showed up during the reaction performed in the presence of BPS is an indication of ferric ion release during the reaction, suggesting that some mNT cluster might be lost (i.e., not transferred to apo-FDX but disassembled). We therefore decided to address in more depth the question of the stoichiometry of the transfer, i.e., the number of [2Fe-2S] mNT clusters consumed to form one [2Fe-2S] cluster in FDX. First, using a native gel, we looked at the proportions of holo- versus apo-mNT in the purified protein we used for the subsequent transfer reactions (Figure 3A) and found that roughly 85% of mNT was in the holo form and 15% in the apo form. Then, we performed cluster transfer experiments for 2 h with a fixed concentration of apo-FDX (40 μM) and increasing concentrations of oxidized mNT and, consequently, increasing oxidized holo-mNT concentrations considering that 85% of mNT was

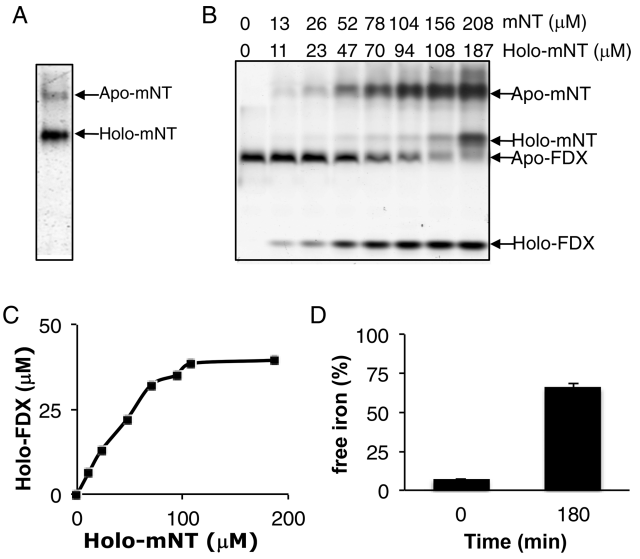

Figure 3. Two mNT clusters were consumed for the formation of only one FDX cluster. (A) Holo-mNT used for this study was run on a 16% reducing native gel. Quantification of the intensity of the bands corresponding to holo- and apo-mNT showed that the protein used in this experiment contained roughly 85% holo form and 15% apo form. (B) Cluster transfer reactions were performed at 25 °C for 2 h in 50 mM Bis-Tris (pH 6.2), 100 mM NaCl, and 0.7 mM DTT under anaerobic conditions with 40 μM apo-FDX and variable concentrations of oxidized holo-mNT. Final reaction products were run on a 16% reducing native gel. Holo-mNT concentrations were estimated from the mNT concentrations (determined by the absorbance at 280 nm as described in Materials and Methods) and the apo-mNT/holo-mNT ratio determined in panel A. (C) For each reaction, concentrations of holo-FDX at the end of the reaction were calculated using the intensity of the bands of apo- and holo-FDX and plotted as a function of the concentration of holo-mNT (i.e., mNT concentration corrected by a factor of 0.85) added during each reaction. The study was performed twice. One representative result is presented. The fit of the linear part (from 0 to 60 μM holo-mNT) indicates that one holo-mNT can form 0.46 ± 0.02 FDX cluster. (D) The cluster transfer reaction was performed at 25 °C for 3 h in 50 mM Bis-Tris (pH 6.2), 100 mM NaCl, and 0.7 mM DTT under anaerobic conditions with 20 μM holo-mNT and apo-FDX. At the beginning (0 min) and end (180 min) of the reaction, free and total irons were quantified as described in Materials and Methods and free iron was expressed as a percentage of total iron. The histogram is the average of three independent experiments.

DOI: 10.1021/acs.biochem.8b00777
Biochemistry XXXX, XXX, XXX−XXX

initially in the holo form (Figure 3B). For each holo-mNT concentration, we quantified the proportion of holo- versus apo-FDX at the end of the reaction (Figure 3C). While the concentration of holo-mNT in the reaction increased, the concentration of holo-FDX at the end of the reaction increased. Even when a large excess of holo-mNT was used, roughly 10% of apo-FDX was not converted to holo-FDX at the end of the reaction, indicating that a portion of apo-FDX is not able to assemble a cluster. Using the slope of the linear part of the curve, we found that 2.2 ± 0.1 holo-mNT clusters (average of two independent series of experiments) are consumed to form one holo-FDX.

In parallel, we quantified the proportion of free iron to total iron at different stages of the cluster transfer reaction. At the beginning of the reaction, we found that 10% of the total iron was free, which correlates well with the 15% of apo-mNT we observed on native gels (Figure 3A). We then performed the same quantification at the end of the cluster transfer reaction performed with equimolar holo-mNT and apo-FDX and found that 60% of the iron was free (Figure 3D). Thus, 50% of the iron bound to mNT at the beginning of the reaction was released in solution at the end of the cluster transfer process. Taken together, these results proved that even if the transfer is direct, roughly two [2Fe-2S] clusters from mNT are consumed for the formation of one [2Fe-2S] cluster in FDX.

Oxidized mNT Is Stable in the Absence of Oxygen Even at Acidic pH. It was previously shown that the stability of oxidized mNT clusters under aerobic conditions is highly dependent on pH, with a decrease in stability with a more acidic pH.[8,40] However, we have recently demonstrated that the presence of O_2 is a major determinant of mNT cluster stability, with oxidized mNT being less stable under aerobic conditions than in the absence of O_2.[17] Thus, we decided to look at the pH dependence of mNT cluster stability under both aerobic and anaerobic conditions by following the absorbance of oxidized holo-mNT at 460 nm over time at 25 °C (Figure 4).[8,23] As previously observed,[8,40] cluster disassembly was clearly pH-dependent under aerobic conditions. We showed that the stability of the oxidized cluster decreases when the pH is more acidic (Figure 4A; $T_{1/2}$ values of 2050 ± 200, 269 ± 69, and 101 ± 6 min at 25 °C and pH 6.7, 6.2, and 5.8, respectively). Interestingly, under anaerobic conditions, the oxidized protein remained highly stable even at acidic pH, with roughly 10% of the clusters lost after 15 h at pH 5.8 and 25 °C (Figure 4B). Nevertheless, it is worth noting that this low pH dependence remained even under anaerobic conditions ($T_{1/2}$ values of roughly 148, 81, and 50 h at 25 °C and pH 6.7, 6.2, and 5.8, respectively), but the amplitude of the dependence is much more limited than under aerobic conditions (the decrease in the pH from 6.7 to 5.8 induces decreases in cluster stability of roughly 20- and 3-fold under aerobic and anaerobic conditions, respectively) (Figure 4A,C). The data demonstrate that under anaerobic conditions the oxidized mNT cluster is more stable than under aerobic conditions and the cluster stability in aerobiosis is highly dependent on pH (with a decrease in cluster stability at a more acidic pH), while in anaerobiosis, the pH dependency persists but is strongly reduced.

To obtain more details about the effect of pH on cluster vicinity, we used electrochemically induced FTIR difference spectra to reveal conformational changes occurring in the protein upon redox state modification. The oxidized minus reduced difference spectra obtained for different pH values

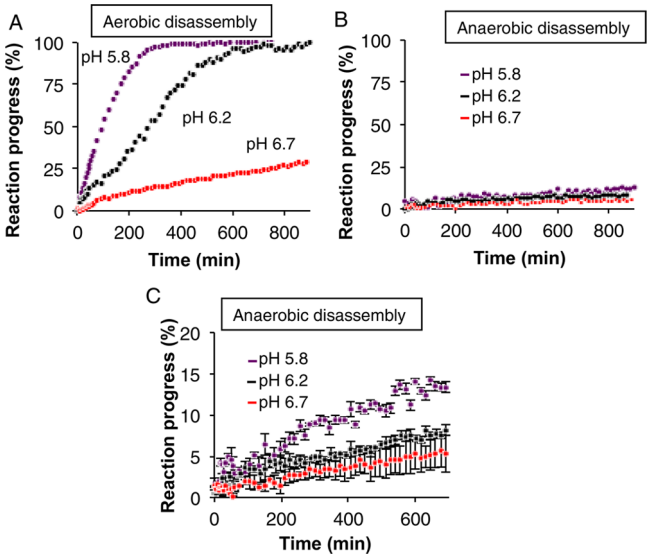

Figure 4. Oxidized mNT cluster is highly stable under anaerobic conditions at 25 °C even at acidic pH. Oxidized mNT cluster loss (20 μM protein) was studied at 25 °C under (A) aerobic or (B and C) anaerobic conditions and followed by UV−vis absorption spectroscopy. The pH of the reaction buffer (50 mM Tris-HCl or Bis-Tris with 100 mM NaCl) was 5.8 (violet), 6.2 (black), and 6.7 (red). For the sake of clarity, either representative experiments (A and B) or average curves with error bars from at least three independent experiments (C) are presented. The reaction progress for each type of reaction was calculated as previously described.[23]

(Figure S1A) revealed a broad differential signal signature that is very similar to those of other proteins with one or more Fe−S clusters[43] and includes the contributions from the ν(C═O) vibration of the backbone, called the amide I signal and seen between 1680 and 1630 cm^{-1}.[44] The experiments performed between pH 8.5 and 5.6 were reversible and stable for a number of redox cycles. At pH 4.8, the signal was lost and redox reaction was no longer possible. Upon comparison of the data for different pH values, the intensity of the amide I signal significantly decreased at more acidic pH values, especially the signal around 1650 cm^{-1}, for the reduced and oxidized forms (see the dotted line in Figure S1A), which suggests conformational changes in the protein. At pH 5.6, the intensities of the signals were significantly reduced. This could be explained by a larger fraction of the protein without a cluster at higher proton concentrations withdrawn from the RedOx reaction.

To identify possible changes in the structure and symmetry of the Fe−S cluster, Raman spectra were recorded between pH 4.8 and 8.5 (Figure S1B). The samples were in the reduced state. At pH 8.5, the Fe−S vibrational modes were seen at 321 cm^{-1}. Between pH 5.6 and 8.5, the signature was essentially conserved. At pH 4.8, changes in the intensity ratio were seen, especially for the signal at 309 cm^{-1}, a shift occurred for the Fe−S vibrational modes from 321 to 328 cm^{-1}, and the signal was greatly broadened. Most likely, the symmetry of the cluster changed because of the loss of at least one ligand. A precise assignment to a specific vibrational mode is difficult, because Raman spectroscopic studies of the naturally occurring $Fe_2S_2(His)(Cys)_3$ motif as found in mNT have been described in only one other protein, a mutant form of the Fe−S scaffold protein IscU.[45] In conclusion, the Raman and infrared spectra both confirm the presence of a [2Fe-2S] cluster between pH

DOI: 10.1021/acs.biochem.8b00777
Biochemistry XXXX, XXX, XXX−XXX

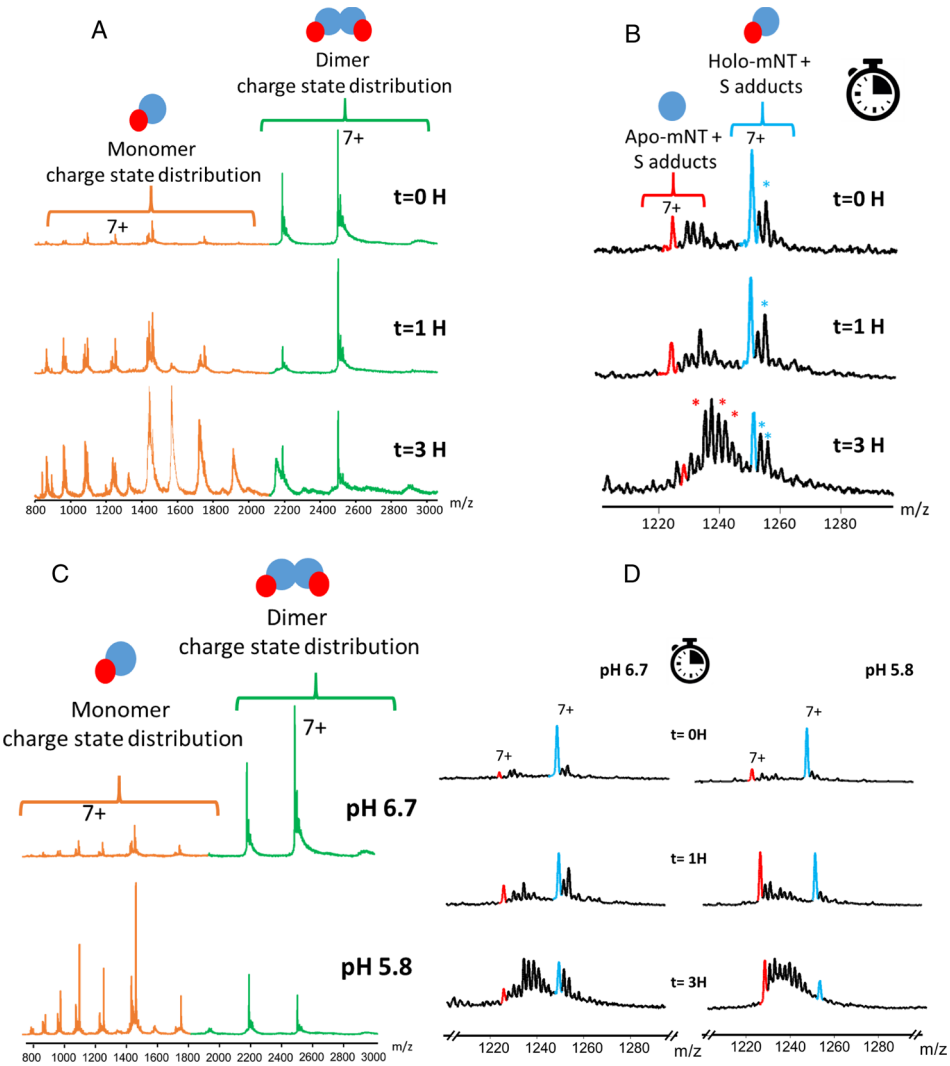

Figure 5. Effect of time and pH on oxidized holo-mNT as monitored by native mass spectrometry. (A and B) Effect of time on the oxidized holo-mNT oligomerization state as monitored by native mass spectrometry. (A) Full scan native mass spectra of a 20 μM injection of oxidized holo-mNT (top) and after incubation for 1 (middle) and 3 h (bottom) at room temperature under aerobic conditions at pH 6.7. Time-dependent mNT dimer destabilization into the mNT monomer was accompanied by [2Fe-2S] cluster loss. (B) Close-up of the 7+ charge state of monomeric mNT at 0 h (top) or after incubation for 1 (middle) and 3 h (bottom). Blue peaks represent holo-mNT, while red peaks refer to apo-mNT. Species labeled with asterisks correspond to nonspecific sulfur adducts as sulfur was present in excess. (C and D) Effect of pH on mNT oligomerization. (C) Full scan native mass spectra of a 20 μM injection of mNT at pH 6.7 (top) and 5.8 (bottom). pH-dependent mNT dimer destabilization into the mNT monomer is accompanied by [2Fe-2S] cluster loss. (D) Close-up of the 7+ charge state of monomeric mNT at 0 h (top) at pH 6.7 (left) and 5.8 (right) or after incubation for 1 (middle) and 3 h (bottom). Blue peaks represent holo-mNT, while red peaks refer to apo-mNT.

5.6 and 8.5, but with small conformational changes around the cofactor.

The Oligomerization State and the Fe−S Cluster of mNT Are Dynamic and Sensitive to pH. To examine the effect of pH on mNT in more depth, we next monitored the effect of time and pH on mNT oligomerization and cluster loss by native MS. We first studied the dynamics of oxidized holo-mNT (20 μM) at pH 6.7 under aerobic conditions and room temperature as a function of time. At time zero, mNT is mostly detected in its noncovalent dimeric form with a mass of 17502.1 ± 0.7 Da, corresponding to two [2Fe-2S] clusters bound to two mNT subunits (Figure 5A, top panel). A minor ion series corresponding to monomeric holo-mNT with one [2Fe-2S] cluster (8751.8 ± 0.2 Da) is also detected in the lower-m/z region (Figure 5A). Native MS experiments next revealed that the ratio of monomeric holo-mNT increases with time (Figure 5A, t = 0, 1, and 3 h). Under strictly identical experimental and instrumental conditions, the relative amount of monomeric species compared to the amount of dimeric species was estimated from the native mass spectral intensities and was shown to increase from 18% at 0 h to 72% after incubation for 3 h at room temperature. We next focused on the monomeric region of the mass spectra to have a closer look at possible [2Fe-2S] cluster loss over time at pH 6.7 (Figure 5B). While holo-mNT is mostly detected at 0 h, signal intensities of ions corresponding to holo-mNT (blue peak in Figure 5B) strongly decrease over time. In parallel, intensities of peaks corresponding to the monomeric apo-mNT signal (red in Figure 5B) and its nonspecific sulfur adducts (labeled with asterisks in Figure 5B) strongly increased. These sulfur adducts could result from binding of released inorganic sulfur due to cluster destabilization to apoprotein, as previously described in the case of several other Fe−S proteins.[41,42] These native MS experiments unambiguously demonstrate that

DOI: 10.1021/acs.biochem.8b00777
Biochemistry XXXX, XXX, XXX−XXX

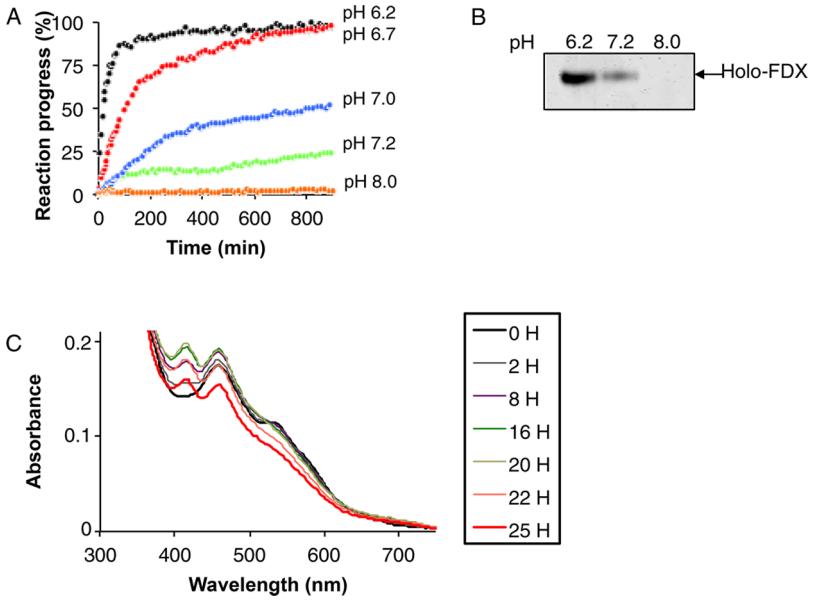

Figure 6. mNT cluster transfer reaction is fast and highly dependent on pH even under anaerobic conditions. mNT cluster transfer (each protein at 20 μM) was performed at 25 °C under anaerobic conditions and followed by either (A) UV−vis absorption spectroscopy or (B) migration on a 16% reducing native gel. The reaction buffer (50 mM Tris-HCl or Bis-Tris with 100 mM NaCl) was at 6.2 (black), 6.7 (red), 7.0 (blue), 7.2 (green), and 8.0 (orange). For the sake of clarity, results of representative experiments are presented. Each experiment was performed at least three times. To avoid mNT cluster reduction, DTT used for apo-FDX reduction was removed with a Micro Bio-Spin column before performing the cluster transfer reaction. Reaction progress for each type of reaction was calculated as previously described.[23] (A and B) mNT cluster transfer under anaerobic conditions followed by UV−vis absorption spectroscopy and migration of the reaction products after reaction for 16 h on a 16% reducing native gel to follow the appearance of holo-FDX, respectively. (C) Kinetics of mNT cluster transfer to apo-FDX at pH 8.0 and 37 °C under anaerobic conditions.

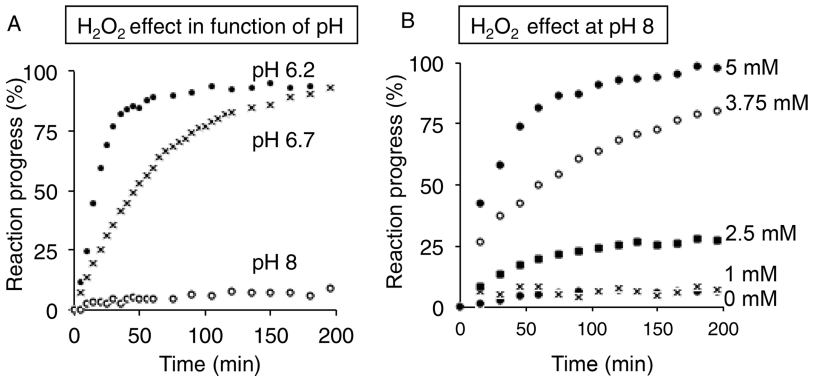

Figure 7. mNT cluster is highly resistant to H_2O_2 *in vitro*. Cluster loss reactions with 20 μM protein were performed at 25 °C under anaerobic conditions and followed by UV−vis absorption spectroscopy. The reaction buffer (50 mM Tris-HCl or Bis-Tris with 100 mM NaCl) was at pH 6.2 (A, ●), 6.7 (A, ×), and 8.0 (A, ○, and B). For the sake of clarity, results of representative experiments are shown. The reaction progress was calculated as previously described.[23] For panel A, 250 μM H_2O_2 was added to mNT at different pHs. (B) Variable concentrations of H_2O_2 were added to mNT at pH 8.0. Each experiment was performed at least thrice.

dimeric holo-mNT is destabilized over time into monomeric apo-mNT with progressive loss of the [2Fe-2S] cluster.

The pH dependency of the oligomerization state of mNT and its cluster disassembly was next investigated (Figure 5C). At 0 h, while mNT is mostly detected in its dimeric holo form at pH 6.7 (Figure 5C, top panel), the ratio of monomeric to dimeric species is fully inverted at pH 5.8 (Figure 5C, bottom panel), highlighting a strong destabilization of mNT dimers into monomers at more acidic pH values. In addition, cluster loss was monitored over time at pH 5.8 (Figure 5D, right panel) and pH 6.7 (Figure 5D, left panel), highlighting faster cluster loss at acidic pH. Thus, pH not only affects cluster stability but also has strong effects on the oligomerization state of holo-mNT, with the dimer becoming less stable at more acidic pH.

The Speed of the Cluster Transfer Reaction Is Highly Modulated by pH. We next looked at the effect of pH on the ability of oxidized holo-mNT to transfer its cluster to apo-FDX *in vitro* using UV−vis absorption spectroscopy (Figure 6A) and migration on a native polyacrylamide gel (Figure 6B) as described previously.[23] O_2 does not affect the speed of the cluster transfer reaction but does affect cluster stability.[17] For this reason, we looked at the effect of pH on the cluster transfer reaction only under anaerobic conditions, which allows us to follow slow reactions without reoxidation of reduced apo-FDX cysteines. At 25 °C, hardly any cluster transfer was observed at pH 8.0 under anaerobic conditions (Figure 6A,B).

DOI: 10.1021/acs.biochem.8b00777
Biochemistry XXXX, XXX, XXX−XXX

However, the speed of mNT cluster transfer increased as the pH became more acidic (at 25 °C, $T_{1/2}$ values of roughly 1800, 810, 100, and 16 min at pH 7.2, 7.0, 6.7, and 6.2, respectively). Thus, at any pH, the cluster transfer reaction was much faster than the cluster disassembly reaction under anaerobic conditions and even under aerobic conditions (compare Figures 4C and 6A). In conclusion, under anaerobic conditions, we showed that cluster disassembly is slow and has a weak pH dependence. In contrast, cluster transfer is faster and highly dependent on pH around physiological values with a roughly 5-fold increase in the speed of the reaction for a decrease of 0.5 pH unit.

Finally, when we increased the temperature of the reaction mixture to 37 °C, holo-FDX formation due to cluster transfer from holo-mNT was observed even at pH 8.0 (Figure 6C), but holo-FDX did not accumulate over time because of its relatively low stability (competition between formation of holo-FDX by cluster transfer from holo-mNT and holo-FDX cluster disassembly at this temperature).

mNT Is Highly Resistant to Hydrogen Peroxide. Previously, we proposed that mNT uses the cluster transfer process to repair the Fe−S cluster of the IRP-1/c-aconitase protein after oxidative stress.[14] For such a cellular function, the mNT cluster has to be particularly resistant to oxidative stress, so we investigated the effect of addition of hydrogen peroxide (H_2O_2) on mNT cluster disassembly *in vitro* under anaerobic conditions, conditions for which mNT is stable for hours at any pH in the absence of H_2O_2. At pH 8, addition of 250 μM H_2O_2 did not significantly destabilize the cluster, but H_2O_2-induced cluster degradation was observed at pH <7 (Figure 7A). Thus, at pH 6.7, the $T_{1/2}$ of oxidized mNT cluster stability was roughly 50 min and decreased when the pH was more acidic, with a $T_{1/2}$ of only 15−20 min at pH 6.2. Finally, we looked at the effects of the addition of H_2O_2 at different doses at pH 8 and found that it has to be added at a concentration of >1 mM to significantly destabilize the cluster (with 2.5 mM H_2O_2, roughly 25% of the cluster was lost after 200 min at 25 °C) (Figure 7B). Thus, addition of H_2O_2 increases the extent of the loss of the mNT cluster, and the effects increase when the pH is more acidic. However, even at pH 6.2, high concentrations of H_2O_2 (250 μM, a >10-fold excess compared to the mNT cluster) have to be used to significantly decrease the stability of the mNT cluster.

DISCUSSION

We have previously demonstrated that reduced holo-mNT is extremely stable and its ability to transfer its cluster is controlled by its own redox state (redox switch).[17] In this study, we pursued this *in vitro* study of mNT cluster transfer to a [2Fe-2S] recipient protein using the gold standard cluster recipient apo-FDX.

In this study, we provide a clear demonstration that the cluster is directly transferred from holo-mNT to the recipient apoprotein as previously observed with other cluster transfer proteins involved in Fe−S cluster biogenesis, such as bacterial SufBCD,[47] SufA,[26] IscU,[48] and plant GRX.[28] This result is compatible with the current molecular model for cluster transfer based on a thiol ligand exchange mechanism,[49] which also implies the formation of a complex, at least transient, between the two proteins as the first step of the reaction. The formation of such a complex has been experimentally demonstrated in several cases (bacterial IscA with FDX[24] or biotin synthase,[50] bacterial SufBCD with SufA,[47] bacterial NfuA with ACNB,[51] GRX from various organisms with IscA[52] or SufA,[53] and human mNT with anamorsin[19]) or suggested by analysis of the kinetic data (ISCU with FDX[25]). In the case of NEET proteins, the interaction between CISD2 and FDX was suggested on the basis of the protein−protein complex docking model and protein cross-linking.[11] Although cluster transfer is direct, we did not observe the formation of a complex between holo-mNT and apo-FDX that is stable enough to be detected by the classic biochemical (pull-down assays) and biophysical (NMR and native mass spectrometry) approaches we tried. Thus, the formation of a stable complex between the donor and acceptor proteins is not mandatory for efficient cluster transfer, and formation of only a transient complex seems to be sufficient. The variety of mNT Fe−S cluster acceptors, including a nonphysiological one, together with nonmandatory strong protein−protein interactions between mNT and the cluster recipient protein may reveal the low substrate specificity of mNT that might thus have the ability to repair a wide range of Fe−S proteins upon oxidative stress.

We found that two mNT [2Fe-2S] clusters are consumed to build one [2Fe-2S] cluster in apo-FDX. Very few similar studies were performed with other cluster transfer proteins. In the case of monothiol GRX, which carries only one cluster per protein dimer, cluster transfer to IscA was stoichiometric.[28,52] Conversely, a 3-fold excess of *Azotobacter vinelandii* IscU was necessary in the case of cluster transfer to AcnA.[48] In our case, holo-mNT is a dimer with one cluster per monomer when holo-FDX is a monomer and carries only one cluster. Our results indicate that there is no concerted cluster transfer from the two subunits of mNT under our experimental conditions. Thus, we propose that after the transfer of one cluster and destructuring of the corresponding mNT subunit polypeptide[14] the remaining holo subunit is cooperatively destabilized due to intermonomer interactions and quickly loses its cluster, as proposed recently by molecular dynamics simulation,[54] before being able to give it to another recipient protein. It might be possible that this low-efficiency cluster transfer could be just a consequence of the use of a nonphysiological cluster recipient protein. Moreover, in the case of a transfer to a [4Fe-4S] cluster recipient protein such as cytosolic aconitase or to a recipient assembling two [2Fe-2S] clusters such as anamorsin, we cannot exclude the possibility that the two clusters of dimeric holo-mNT are transferred in a concerted reaction to transfer them as [2Fe-2S] clusters (anamorsin) or use them to build up a [4Fe-4S] cluster (aconitase).

Holo-mNT is extremely resistant to hydrogen peroxide *in vitro* compared to other cluster transfer proteins. It is known that bacterial IscU, the scaffold protein involved in Fe−S cluster maturation, is less stable than SufB, a protein involved in an alternative pathway used by bacteria when stress occurs ($T_{1/2}$ values of <5 and $\lesssim$10 min, respectively, when 70 equiv of H_2O_2 was added to the protein at pH 8.0 and 25 °C under anaerobic conditions).[55] Under exactly the same conditions, the mNT cluster was only slightly degraded by addition of H_2O_2. This high resistance of mNT to H_2O_2 is compatible with its redox switch behavior and its involvement in the cellular response after oxidative stress as we proposed previously.[14]

mNT cluster lability is known to be pH-dependent (increased lability as the pH decreases) under aerobic conditions.[8] The protonation of N_ε of His87 (pK_a of ∼6.5) at low pH is at least partially responsible for this behavior by

DOI: 10.1021/acs.biochem.8b00777
Biochemistry XXXX, XXX, XXX−XXX

decreasing the energy required for Fe−N_δ bond cleavage.[46,54,56] Clearly, the conserved hydrogen-bonding network around the mNT cluster also contributed to this pH sensitivity.[40] Interestingly, we confirmed the strong pH sensitivity under aerobic conditions and found that mNT is much less sensitive to pH under anaerobic conditions. Thus, pH only slightly affects the inherent stability of the mNT cluster but does strongly modulate its sensitivity to O_2 (or to related derived species).

Our studies reveal that pH also affects the dimerization of the protein, with the dimer being less stable at acidic pH. Interestingly, structural analysis has shown that even if mNT dimerization is mainly mediated by hydrophobic interactions, the dimer interface is stabilized by interprotomer hydrogen bonds between His58 and Arg73 and the presence of two buried water molecules.[5,6] Thus, the mNT dimer is less stable at acidic pH. NMR studies revealed only two structural protein states involving either the dimeric folded holoprotein or the unfolded mNT resulting from cluster loss. The current NMR data[14] suggest that several resonances are invisible around cysteine residues in the unfolded state. Hence, it is highly probable that the unfolded state seen by NMR can be bound to iron−sulfur species or in the apo form with intermediate exchange-induced line broadening. Native MS studies suggest that mNT might exist as a dimeric holo-mNT form or as monomeric holo- or apo-mNT forms. We can conclude that mNT monomers do not exist with a stable three-dimensional fold and might rapidly unfold, while keeping or losing the ability to bind iron−sulfur species.

The cluster transfer reaction is also clearly pH-dependent under anaerobic conditions. In the cluster transfer molecular model based on thiol ligand exchanges, the first Fe−$ligand_{donor}$ has to be broken to form the first Fe−$ligand_{acceptor}$. Thus, the Fe−N_δ bond (His87) has to be attacked by a thiol group of the recipient protein to initiate cluster transfer instead of an exogenous O_2 molecule as for cluster stability under aerobic conditions. If this bond is extremely stable (the case of the H87C mutated form with a cluster fully coordinated by cysteines), it cannot be broken by O_2 or by a thiol group of the recipient protein, and this form cannot lose or transfer its cluster. For the WT form, when the pH is more acidic, the bond between Fe and N_δ (His87) is more easily broken by O_2 or by a thiol group of the recipient protein due to protonation of the histidine but also probably due to modification of the hydrogen bond network around the cluster.[40] Then, at acidic pH, the cluster is less stable under aerobic conditions and more easily transferred to a recipient protein regardless of the presence of O_2. In conclusion, this pH sensitivity allows mNT to regulate very finely its ability to transfer its cluster as a function of pH. This property differentiates mNT from other cluster transfer proteins such as IscU, whose conflicting coordination of its cluster by two residues (D39 and H105 in *Escherichia coli* IscU) seems to induce cluster instability.[57]

The cytoplasmic pH (pH_i) has been implicated in the control of several vital cellular functions and cell fate. In resting cells, pH_i is tightly and dynamically regulated to near neutral values (7.0−7.2) and some cellular events can affect this intracellular acid−base homeostasis.[58] Thus, early apoptotic events induce rapid cytosol acidification to pH 6.3−6.8 followed by cytochrome *c* release and optimal caspase activation.[59] Conversely, invasive tumor cells have a more alkaline baseline pH_i around 7.2−7.8 that protects them from entering the apoptotic cascade.[60] Finally, large pathophysiological acid−base disturbances have also been observed in heart diseases such as myocardial ischemia,[61] in the early stages of tumorigenesis, and in neurodegenerative diseases, including Alzheimer's and Parkinson's diseases.[62] Thus, the results of our *in vitro* studies demonstrate that the ability of mNT to transfer its cluster is very sensitive to pH below pH 7 when more alkaline pH values seriously impair it. We propose that mNT could act not only as a redox switch but also as a pH_i sensor that may control some cellular pathways in response to physiological variations in cellular pH. Thus, when pathophysiological conditions such as cancer or neurodegenerative diseases would dysregulate cellular pH_i homeostasis, the pH regulation of mNT would be disturbed. Finally, voltage-dependent anion channel type 1 (VDAC1), which is a crucial channel for mitochondrial metabolism regulation and is involved in the early steps of apoptosis, is also known to be sensitive to cytosolic pH_i variation.[63] We demonstrated recently that depletion of the endoplasmic reticulum-localized NEET protein CISD2 leads to C-terminal cleavage of VDAC1,[64] results that established a functional link between VDAC1 and CISD2, a potential interactant of mNT.[20]

SUMMARY AND CONCLUSIONS

It was demonstrated before that mNT is an Fe−S protein capable of transferring its cluster to repair stress-damaged Fe−S proteins. This cluster transfer is clearly under the control of the redox state of mNT's cluster (redox switch). Here we demonstrated that mNT is a highly stable Fe−S cluster to H_2O_2 compared to other known Fe−S cluster proteins. Moreover, not only the cluster stability but also the protein dimerization and, maybe even more importantly, the ability of mNT to transfer its cluster are finely regulated by the pH around physiological pH values. We propose that mNT may act as a pH sensor to regulate cellular pathways in response to oxidative stress and cellular pH variations.

ASSOCIATED CONTENT

Supporting Information

The Supporting Information is available free of charge on the ACS Publications website at DOI: 10.1021/acs.biochem.8b00777.

Figure S1 (PDF)

AUTHOR INFORMATION

Corresponding Author

*Institut de Chimie des Substances Naturelles, UPR 2301-CNRS, 1 avenue de la Terrasse, 91190 Gif-sur-Yvette, France. E-mail: marie-pierre.golinelli@cnrs.fr. Telephone: (33) 1 69 82 30 12. Fax: (33) 1 69 07 72 47.

ORCID

Sarah Cianférani: 0000-0003-4013-4129

Marie-Pierre Golinelli-Cohen: 0000-0002-6738-8631

Funding

This work was supported by the CNRS, the University of Strasbourg, the "Agence Nationale de la Recherche" (ANR-13-BSV8-0017-01), and the French Proteomic Infrastructure (ProFI; ANR-10-INBS-08-03). T.B. acknowledges the Institut de Recherches Internationales Servier for funding of his Ph.D. fellowship.

Notes

The authors declare no competing financial interest.

DOI: 10.1021/acs.biochem.8b00777
Biochemistry XXXX, XXX, XXX−XXX

■ ACKNOWLEDGMENTS

The authors acknowledge the IMAGIF cloning platform (CNRS, Gif-sur-Yvette, France). The authors also warmly acknowledge the networking support from the EU COST Action FeSBioNet (CA15133).

■ ABBREVIATIONS

BPS, bathophenanthroline sulfonate; BSA, bovine serum albumin; c-aconitase, cytosolic aconitase; DTT, dithiothreitol; EDTA, ethylenediaminetetraacetic acid; ESI-MS, electrospray ionization mass spectrometry; FDX, *E. coli* [2Fe-2S] ferredoxin; FTIR, Fourier transform infrared spectroscopy; IRP-1, iron regulatory protein 1; mNT, mitoNEET; MS, mass spectrometry; NMR, nuclear magnetic resonance; OMM, outer mitochondrial membrane; SOFAST-HMQC, band-selective optimized flip angle short transient heteronuclear multiple-quantum correlation; WT, wild type

■ REFERENCES

(1) Beinert, H. (2000) Iron-sulfur proteins: ancient structures, still full of surprises. *JBIC, J. Biol. Inorg. Chem. 5*, 2−15.

(2) Johnson, D. C., Dean, D. R., Smith, A. D., and Johnson, M. K. (2005) Structure, function, and formation of biological iron-sulfur clusters. *Annu. Rev. Biochem. 74*, 247−281.

(3) Heidrich, H. G., Albracht, S. P., and Backstrom, D. (1978) Two iron-sulfur centers in mitochondrial outer membranes from beef heart as prepared by free-flow electrophoresis. *FEBS Lett. 95*, 314−318.

(4) Wiley, S. E., Murphy, A. N., Ross, S. A., van der Geer, P., and Dixon, J. E. (2007) MitoNEET is an iron-containing outer mitochondrial membrane protein that regulates oxidative capacity. *Proc. Natl. Acad. Sci. U. S. A. 104*, 5318−5323.

(5) Paddock, M. L., Wiley, S. E., Axelrod, H. L., Cohen, A. E., Roy, M., Abresch, E. C., Capraro, D., Murphy, A. N., Nechushtai, R., Dixon, J. E., and Jennings, P. A. (2007) MitoNEET is a uniquely folded 2Fe 2S outer mitochondrial membrane protein stabilized by pioglitazone. *Proc. Natl. Acad. Sci. U. S. A. 104*, 14342−14347.

(6) Hou, X., Liu, R., Ross, S., Smart, E. J., Zhu, H., and Gong, W. (2007) Crystallographic studies of human MitoNEET. *J. Biol. Chem. 282*, 33242−33246.

(7) Lin, J., Zhou, T., Ye, K., and Wang, J. (2007) Crystal structure of human mitoNEET reveals distinct groups of iron sulfur proteins. *Proc. Natl. Acad. Sci. U. S. A. 104*, 14640−14645.

(8) Wiley, S. E., Paddock, M. L., Abresch, E. C., Gross, L., van der Geer, P., Nechushtai, R., Murphy, A. N., Jennings, P. A., and Dixon, J. E. (2007) The outer mitochondrial membrane protein mitoNEET contains a novel redox-active 2Fe-2S cluster. *J. Biol. Chem. 282*, 23745−23749.

(9) Conlan, A. R., Axelrod, H. L., Cohen, A. E., Abresch, E. C., Zuris, J., Yee, D., Nechushtai, R., Jennings, P. A., and Paddock, M. L. (2009) Crystal structure of Miner1: The redox-active 2Fe-2S protein causative in Wolfram Syndrome 2. *J. Mol. Biol. 392*, 143−153.

(10) Inupakutika, M. A., Sengupta, S., Nechushtai, R., Jennings, P. A., Onuchic, J. N., Azad, R. K., Padilla, P., and Mittler, R. (2017) Phylogenetic analysis of eukaryotic NEET proteins uncovers a link between a key gene duplication event and the evolution of vertebrates. *Sci. Rep. 7*, 42571.

(11) Tamir, S., Paddock, M. L., Darash-Yahana-Baram, M., Holt, S. H., Sohn, Y. S., Agranat, L., Michaeli, D., Stofleth, J. T., Lipper, C. H., Morcos, F., Cabantchik, I. Z., Onuchic, J. N., Jennings, P. A., Mittler, R., and Nechushtai, R. (2015) Structure-function analysis of NEET proteins uncovers their role as key regulators of iron and ROS homeostasis in health and disease. *Biochim. Biophys. Acta, Mol. Cell Res. 1853*, 1294−1315.

(12) Nechushtai, R., Conlan, A. R., Harir, Y., Song, L., Yogev, O., Eisenberg-Domovich, Y., Livnah, O., Michaeli, D., Rosen, R., Ma, V., Luo, Y., Zuris, J. A., Paddock, M. L., Cabantchik, Z. I., Jennings, P. A., and Mittler, R. (2012) Characterization of Arabidopsis NEET reveals an ancient role for NEET proteins in iron metabolism. *Plant Cell 24*, 2139−2154.

(13) Kusminski, C. M., Holland, W. L., Sun, K., Park, J., Spurgin, S. B., Lin, Y., Askew, G. R., Simcox, J. A., McClain, D. A., Li, C., and Scherer, P. E. (2012) MitoNEET-driven alterations in adipocyte mitochondrial activity reveal a crucial adaptive process that preserves insulin sensitivity in obesity. *Nat. Med. 18*, 1539−1549.

(14) Ferecatu, I., Gonçalves, S., Golinelli-Cohen, M.-P., Clémancey, M., Martelli, A., Riquier, S., Guittet, E., Latour, J.-M., Puccio, H., Drapier, J.-C., Lescop, E., and Bouton, C. (2014) The Diabetes Drug Target MitoNEET Governs a Novel Trafficking Pathway to Rebuild an Fe-S Cluster into Cytosolic Aconitase/Iron Regulatory Protein 1. *J. Biol. Chem. 289*, 28070−28086.

(15) Moreno-Navarrete, J. M., Moreno, M., Ortega, F., Sabater, M., Xifra, G., Ricart, W., and Fernandez-Real, J. M. (2016) CISD1 in association with obesity-associated dysfunctional adipogenesis in human visceral adipose tissue. *Obesity 24*, 139−147.

(16) Sohn, Y. S., Tamir, S., Song, L., Michaeli, D., Matouk, I., Conlan, A. R., Harir, Y., Holt, S. H., Shulaev, V., Paddock, M. L., Hochberg, A., Cabanchick, I. Z., Onuchic, J. N., Jennings, P. A., Nechushtai, R., and Mittler, R. (2013) NAF-1 and mitoNEET are central to human breast cancer proliferation by maintaining mitochondrial homeostasis and promoting tumor growth. *Proc. Natl. Acad. Sci. U. S. A. 110*, 14676−14681.

(17) Golinelli-Cohen, M.-P., Lescop, E., Mons, C., Goncalves, S., Clemancey, M., Santolini, J., Guittet, E., Blondin, G., Latour, J.-M., and Bouton, C. (2016) Redox Control of the Human Iron-Sulfur Repair Protein MitoNEET Activity via its Iron-Sulfur Cluster. *J. Biol. Chem. 291*, 7583−7593.

(18) Zuris, J. A., Harir, Y., Conlan, A. R., Shvartsman, M., Michaeli, D., Tamir, S., Paddock, M. L., Onuchic, J. N., Mittler, R., Cabantchik, Z. I., Jennings, P. A., and Nechushtai, R. (2011) Facile transfer of [2Fe-2S] clusters from the diabetes drug target mitoNEET to an apo-acceptor protein. *Proc. Natl. Acad. Sci. U. S. A. 108*, 13047−13052.

(19) Lipper, C. H., Paddock, M. L., Onuchic, J. N., Mittler, R., Nechushtai, R., and Jennings, P. A. (2015) Cancer-Related NEET Proteins Transfer 2Fe-2S Clusters to Anamorsin, a Protein Required for Cytosolic Iron-Sulfur Cluster Biogenesis. *PLoS One 10*, e0139699.

(20) Karmi, O., Holt, S. H., Song, L., Tamir, S., Luo, Y., Bai, F., Adenwalla, A., Darash-Yahana, M., Sohn, Y. S., Jennings, P. A., Azad, R. K., Onuchic, J. N., Morcos, F., Nechushtai, R., and Mittler, R. (2017) Interactions between mitoNEET and NAF-1 in cells. *PLoS One 12*, e0175796.

(21) Golinelli-Cohen, M.-P., and Bouton, C. (2017) Fe-S Proteins Acting as Redox Switch: New Key Actors of Cellular Adaptive Responses. *Curr. Chem. Biol. 11*, 70−88.

(22) Camponeschi, F., Ciofi-Baffoni, S., and Banci, L. (2017) Anamorsin/Ndor1 Complex Reduces [2Fe-2S]-MitoNEET via a Transient Protein-Protein Interaction. *J. Am. Chem. Soc. 139*, 9479−9482.

(23) Mons, C., Ferecatu, I., Riquier, S., Lescop, E., Bouton, C., and Golinelli-Cohen, M.-P. (2017) Combined biochemical, biophysical and cellular methods to study Fe-S cluster transfer and cytosolic aconitase repair by mitoNEET. *Methods Enzymol. 595*, 83−106.

(24) Ollagnier-de-Choudens, S., Mattioli, T., Takahashi, Y., and Fontecave, M. (2001) Iron-sulfur cluster assembly: characterization of IscA and evidence for a specific and functional complex with ferredoxin. *J. Biol. Chem. 276*, 22604−22607.

(25) Wu, S. P., Mansy, S. S., and Cowan, J. A. (2005) Iron-sulfur cluster biosynthesis. Molecular chaperone DnaK promotes IscU-bound [2Fe-2S] cluster stability and inhibits cluster transfer activity. *Biochemistry 44*, 4284−4293.

(26) Gupta, V., Sendra, M., Naik, S. G., Chahal, H. K., Huynh, B. H., Outten, F. W., Fontecave, M., and Ollagnier de Choudens, S. (2009) Native Escherichia coli SufA, coexpressed with SufBCDSE, purifies as a [2Fe-2S] protein and acts as an Fe-S transporter to Fe-S target enzymes. *J. Am. Chem. Soc. 131*, 6149−6153.

DOI: 10.1021/acs.biochem.8b00777
Biochemistry XXXX, XXX, XXX−XXX

(27) Chandramouli, K., and Johnson, M. K. (2006) HscA and HscB stimulate [2Fe-2S] cluster transfer from IscU to apoferredoxin in an ATP-dependent reaction. *Biochemistry 45*, 11087−11095.
(28) Bandyopadhyay, S., Gama, F., Molina-Navarro, M. M., Gualberto, J. M., Claxton, R., Naik, S. G., Huynh, B. H., Herrero, E., Jacquot, J. P., Johnson, M. K., and Rouhier, N. (2008) Chloroplast monothiol glutaredoxins as scaffold proteins for the assembly and delivery of [2Fe-2S] clusters. *EMBO J. 27*, 1122−1133.
(29) Chahal, H. K., and Outten, F. W. (2012) Separate FeS scaffold and carrier functions for SufB(2)C(2) and SufA during in vitro maturation of [2Fe2S] Fdx. *J. Inorg. Biochem. 116*, 126−134.
(30) Sen, S., and Cowan, J. A. (2017) Role of protein-glutathione contacts in defining glutaredoxin-3 [2Fe-2S] cluster chirality, ligand exchange and transfer chemistry. *JBIC, J. Biol. Inorg. Chem. 22*, 1075−1087.
(31) Bradford, M. M. (1976) A rapid and sensitive method for the quantitation of microgram quantities of protein utilizing the principle of protein-dye binding. *Anal. Biochem. 72*, 248−254.
(32) Schanda, P., Kupce, E., and Brutscher, B. (2005) SOFAST-HMQC experiments for recording two-dimensional heteronuclear correlation spectra of proteins within a few seconds. *J. Biomol. NMR 33*, 199−211.
(33) Fish, W. W. (1988) Rapid colorimetric micromethod for the quantitation of complexed iron in biological samples. *Methods Enzymol. 158*, 357−364.
(34) Moulis, J. M., and Meyer, J. (1982) Characterization of the selenium-substituted 2 [4Fe-4Se] ferredoxin from Clostridium pasteurianum. *Biochemistry 21*, 4762−4771.
(35) Moss, D., Nabedryk, E., Breton, J., and Mantele, W. (1990) Redox-linked conformational changes in proteins detected by a combination of infrared spectroscopy and protein electrochemistry. Evaluation of the technique with cytochrome c. *Eur. J. Biochem. 187*, 565−572.
(36) Hellwig, P., Scheide, D., Bungert, S., Mantele, W., and Friedrich, T. (2000) FT-IR spectroscopic characterization of NADH:ubiquinone oxidoreductase (complex I) from Escherichia coli: oxidation of FeS cluster N2 is coupled with the protonation of an aspartate or glutamate side chain. *Biochemistry 39*, 10884−10891.
(37) Kaltashov, I. A., Zhang, M., Eyles, S. J., and Abzalimov, R. R. (2006) Investigation of structure, dynamics and function of metalloproteins with electrospray ionization mass spectrometry. *Anal. Bioanal. Chem. 386*, 472−481.
(38) Hernandez, H., and Robinson, C. V. (2001) Dynamic protein complexes: insights from mass spectrometry. *J. Biol. Chem. 276*, 46685−46688.
(39) Marcoux, J., and Cianferani, S. (2015) Towards integrative structural mass spectrometry: Benefits from hybrid approaches. *Methods 89*, 4−12.
(40) Bak, D. W., and Elliott, S. J. (2013) Conserved hydrogen bonding networks of MitoNEET tune Fe-S cluster binding and structural stability. *Biochemistry 52*, 4687−4696.
(41) Crack, J. C., Thomson, A. J., and Le Brun, N. E. (2017) Mass spectrometric identification of intermediates in the O2-driven [4Fe-4S] to [2Fe-2S] cluster conversion in FNR. *Proc. Natl. Acad. Sci. U. S. A. 114*, E3215−E3223.
(42) Kennedy, M. C., and Beinert, H. (1988) The state of cluster SH and S2- of aconitase during cluster interconversions and removal. A convenient preparation of apoenzyme. *J. Biol. Chem. 263*, 8194−8198.
(43) Friedrich, T., and Hellwig, P. (2010) Redox-induced conformational changes within the Escherichia coli NADH ubiquinone oxidoreductase (complex I): an analysis by mutagenesis and FT-IR spectroscopy. *Biochim. Biophys. Acta, Bioenerg. 1797*, 659−663.
(44) Barth, A. (2007) Infrared spectroscopy of proteins. *Biochim. Biophys. Acta, Bioenerg. 1767*, 1073−1101.
(45) Shimomura, Y., Wada, K., Fukuyama, K., and Takahashi, Y. (2008) The asymmetric trimeric architecture of [2Fe-2S] IscU: implications for its scaffolding during iron-sulfur cluster biosynthesis. *J. Mol. Biol. 383*, 133−143.
(46) Tirrell, T. F., Paddock, M. L., Conlan, A. R., Smoll, E. J., Jr., Nechushtai, R., Jennings, P. A., and Kim, J. E. (2009) Resonance Raman studies of the (His)(Cys)3 2Fe-2S cluster of MitoNEET: comparison to the (Cys)4 mutant and implications of the effects of pH on the labile metal center. *Biochemistry 48*, 4747−4752.
(47) Chahal, H. K., Dai, Y., Saini, A., Ayala-Castro, C., and Outten, F. W. (2009) The SufBCD Fe-S scaffold complex interacts with SufA for Fe-S cluster transfer. *Biochemistry 48*, 10644−10653.
(48) Unciuleac, M. C., Chandramouli, K., Naik, S., Mayer, S., Huynh, B. H., Johnson, M. K., and Dean, D. R. (2007) In vitro activation of apo-aconitase using a [4Fe-4S] cluster-loaded form of the IscU [Fe-S] cluster scaffolding protein. *Biochemistry 46*, 6812−6821.
(49) Fontecave, M., and Ollagnier-de-Choudens, S. (2008) Iron-sulfur cluster biosynthesis in bacteria: Mechanisms of cluster assembly and transfer. *Arch. Biochem. Biophys. 474*, 226−237.
(50) Ollagnier-de-Choudens, S., Sanakis, Y., and Fontecave, M. (2004) SufA/IscA: reactivity studies of a class of scaffold proteins involved in [Fe-S] cluster assembly. *JBIC, J. Biol. Inorg. Chem. 9*, 828−838.
(51) Py, B., Gerez, C., Angelini, S., Planel, R., Vinella, D., Loiseau, L., Talla, E., Brochier-Armanet, C., Garcia Serres, R., Latour, J. M., Ollagnier-de Choudens, S., Fontecave, M., and Barras, F. (2012) Molecular organization, biochemical function, cellular role and evolution of NfuA, an atypical Fe-S carrier. *Mol. Microbiol. 86*, 155−171.
(52) Banci, L., Brancaccio, D., Ciofi-Baffoni, S., Del Conte, R., Gadepalli, R., Mikolajczyk, M., Neri, S., Piccioli, M., and Winkelmann, J. (2014) [2Fe-2S] cluster transfer in iron-sulfur protein biogenesis. *Proc. Natl. Acad. Sci. U. S. A. 111*, 6203−6208.
(53) Mapolelo, D. T., Zhang, B., Randeniya, S., Albetel, A. N., Li, H., Couturier, J., Outten, C. E., Rouhier, N., and Johnson, M. K. (2013) Monothiol glutaredoxins and A-type proteins: partners in Fe-S cluster trafficking. *Dalton Trans. 42*, 3107−3115.
(54) Pesce, L., Calandrini, V., Marjault, H. B., Lipper, C. H., Rossetti, G., Mittler, R., Jennings, P. A., Bauer, A., Nechushtai, R., and Carloni, P. (2017) Molecular Dynamics Simulations of the [2Fe-2S] Cluster-Binding Domain of NEET Proteins Reveal Key Molecular Determinants That Induce Their Cluster Transfer/Release. *J. Phys. Chem. B 121*, 10648−10656.
(55) Blanc, B., Clemancey, M., Latour, J. M., Fontecave, M., and Ollagnier de Choudens, S. (2014) Molecular investigation of iron-sulfur cluster assembly scaffolds under stress. *Biochemistry 53*, 7867−7869.
(56) Bak, D. W., Zuris, J. A., Paddock, M. L., Jennings, P. A., and Elliott, S. J. (2009) Redox characterization of the FeS protein MitoNEET and impact of thiazolidinedione drug binding. *Biochemistry 48*, 10193−10195.
(57) Adrover, M., Howes, B. D., Iannuzzi, C., Smulevich, G., and Pastore, A. (2015) Anatomy of an iron-sulfur cluster scaffold protein: Understanding the determinants of [2Fe-2S] cluster stability on IscU. *Biochim. Biophys. Acta, Mol. Cell Res. 1853*, 1448−1456.
(58) White, K. A., Grillo-Hill, B. K., and Barber, D. L. (2017) Cancer cell behaviors mediated by dysregulated pH dynamics at a glance. *J. Cell Sci. 130*, 663−669.
(59) Matsuyama, S., Llopis, J., Deveraux, Q. L., Tsien, R. Y., and Reed, J. C. (2000) Changes in intramitochondrial and cytosolic pH: early events that modulate caspase activation during apoptosis. *Nat. Cell Biol. 2*, 318−325.
(60) Harguindey, S., Stanciu, D., Devesa, J., Alfarouk, K., Cardone, R. A., Polo Orozco, J. D., Devesa, P., Rauch, C., Orive, G., Anitua, E., Roger, S., and Reshkin, S. J. (2017) Cellular acidification as a new approach to cancer treatment and to the understanding and therapeutics of neurodegenerative diseases. *Semin. Cancer Biol. 43*, 157−179.
(61) Vaughan-Jones, R. D., Spitzer, K. W., and Swietach, P. (2009) Intracellular pH regulation in heart. *J. Mol. Cell. Cardiol. 46*, 318−331.

DOI: 10.1021/acs.biochem.8b00777
Biochemistry XXXX, XXX, XXX−XXX

(62) Ruffin, V. A., Salameh, A. I., Boron, W. F., and Parker, M. D. (2014) Intracellular pH regulation by acid-base transporters in mammalian neurons. *Front. Physiol. 5*, 43.
(63) Teijido, O., Rappaport, S. M., Chamberlin, A., Noskov, S. Y., Aguilella, V. M., Rostovtseva, T. K., and Bezrukov, S. M. (2014) Acidification asymmetrically affects voltage-dependent anion channel implicating the involvement of salt bridges. *J. Biol. Chem. 289*, 23670−23682.
(64) Ferecatu, I., Canal, F., Fabbri, L., Mazure, N., Bouton, C., and Golinelli-Cohen, M.-P. (2018) Dysfunction in the mitochondrial Fe-S assembly machinery leads to the formation of the chemoresistant truncated VDAC1 isoform without HIF1-α activation. *PLoS One 13*, e0194782.

DOI: 10.1021/acs.biochem.8b00777
Biochemistry XXXX, XXX, XXX−XXX